

Spectral prediction model for color prints on paper with fluorescent additives

Roger David Hersch

School for Computer and Communications Sciences, Ecole Polytechnique Fédérale de Lausanne (EPFL),
1015 Lausanne, Switzerland (rd.hersch@epfl.ch)

Received 7 August 2008; revised 4 November 2008; accepted 5 November 2008;
posted 11 November 2008 (Doc. ID 99892); published 12 December 2008

I propose a model for predicting the total reflectance of color halftones printed on paper incorporating fluorescent brighteners. The total reflectance is modeled as the additive superposition of the relative fluorescent emission and the pure reflectance of the color print. The fluorescent emission prediction model accounts for both the attenuation of light by the halftone within the excitation wavelength range and for the attenuation of the fluorescent emission by the same halftone within the emission wavelength range. The model's calibration relies on reflectance measurements of the optically brightened paper and of the solid colorant patches with two illuminants, one including and one excluding the UV components. The part of the model predicting the pure reflectance relies on an ink-spreading extended Clapper–Yule model. On uniformly distributed surface coverages of cyan, magenta, and yellow halftone patches, the proposed model predicts the relative fluorescent emission with a high accuracy (mean $\Delta E_{94} = 0.42$ under a D65 standard illuminant). For optically brightened paper exhibiting a moderate fluorescence, the total reflectance prediction improves the spectral reflectance prediction mainly for high-light color halftones, comprising a proportion of paper white above 12%. Applications include the creation of improved printer characterization tables for color management purposes and the prediction of color gamuts for new combinations of optically brightened papers and inks. © 2008 Optical Society of America

OCIS codes: 100.2810, 260.2510, 330.1710.

1. Introduction

A variety of models exists for predicting the color of cyan, magenta, yellow, and black halftones printed on paper [1–6]. Since these models ignore the influence of the paper fluorescence, their prediction accuracy may be limited, especially for color halftones printed on paper incorporating fluorescent brighteners. The color of these prints depends on whether the illuminant includes or excludes UV light components [7,8].

In the present contribution, I propose a comprehensive spectral prediction model accounting for the paper fluorescence. The model is in the same category as the classical Clapper–Yule multiple reflection model [9], enhanced in order to account for ink spreading [5]. It requires for its calibration only

a spectrophotometer capable of performing reflectance measurements in the wavelength range between 380 and 730 nm under two illuminants, one with UV included and one with UV excluded.

In order to compute the relative irradiance of light emitted by fluorescence, I first develop the equations allowing us to compute the attenuation of incident light within the excitation wavelength range (UV) due to the print's color halftone layer. This attenuation of incident light is mainly due to the transmittances of the inks forming the color halftone and to the portion of incident UV light components reflected by the optically brightened paper and refracted into the air.

The attenuated incident light within the excitation range, absorbed by the paper bulk, moves the fluorescent molecules from a ground energy state E_0 into the vibrational levels of a higher energy state E_1 ([10], pp. 70–71). The intensity of the fluorescent

emission spectrum is proportional to the absorbed energy. The shape of the fluorescent emission spectrum is independent of the absorbed energy ([11], pp. 205–207). The upward traveling irradiance emitted from the paper bulk is attenuated by the multiple reflections between the print–air interface and the paper bulk. The emitted attenuated irradiance emerging from the print–air interface forms the exiting fluorescent irradiance. The total reflectance of the print is the ratio of the total exiting irradiance to the incident irradiance. The total exiting irradiance is formed by the sum of the exiting fluorescent irradiance and of the irradiance reflected by the print without fluorescence.

In Section 2 I review previous work. In Section 3 I introduce the Clapper–Yule model that describes the reflectance of color halftone prints without accounting for the fluorescence phenomenon. In Section 4 I introduce the ink-spreading model that enables us, in conjunction with the Clapper–Yule model, to provide accurate spectral reflectance predictions. In Section 5 I model the attenuation of incident light components in the UV wavelength range. In Section 6 I calculate how much of the light emitted by the fluorescent brighteners within the paper bulk exits the halftone print. In Section 7 I establish the model predicting both the relative fluorescent emission and the total reflectance of color halftones printed on optically brightened paper and show how to calibrate the model’s parameters. In Section 8 I present the results and the achieved prediction accuracy. In Section 9 I draw the conclusions.

2. Previous Work

Basic work performed in the fifties and sixties of the twentieth century related to fluorescent brighteners and to the fluorescence of papers and inks is summarized by Grum [12]. The Donaldson fluorescence matrix describes the emission intensities at discrete emission wavelengths as a function of the incident light intensities at discrete excitation wavelengths [13]. The deduction of the matrix coefficients requires a fluorescence spectrophotometer performing the spectral decomposition both of the illuminant and of the light reflected by the fluorescent sample. The Donaldson fluorescence matrix enables computing the pure reflectance and the emitted fluorescence spectrum of a fluorescent sample according to the spectral distribution of the illuminant. Alternative methods exist to deduce the pure reflectance of a fluorescent substrate by performing several spectral measurements under different illuminants [14].

Most fluorescent models rely on the superposition paradigm: light apparently reflected by a fluorescent substrate is the light reflected by that substrate without fluorescence plus the light emitted by fluorescence. Therefore the total reflectance $R_{\text{total}}(\lambda)$ of a paper with fluorescent additives is the ratio of the sum of the purely reflected irradiance $I_0(\lambda) \times R_{\text{pure}}$ of the paper illuminated by a light source $I_0(\lambda)$ excluding UV components and the emitted fluorescent

irradiance $F(\lambda)$ when illuminated with the same light source including UV components to the incident irradiance $I_0(\lambda)$:

$$R_{\text{total}}(\lambda) = \frac{F(\lambda) + I_0(\lambda) \cdot R_{\text{pure}}(\lambda)}{I_0(\lambda)} = \frac{F(\lambda)}{I_0(\lambda)} + R_{\text{pure}}(\lambda). \quad (1)$$

Recent spectral prediction models dealing with the fluorescence phenomenon were focussed mainly on the fluorescence of inks [15–17]. They rely on a two-flux approach similar to the Kubelka–Munk theory. They assume that within an infinitesimally thin portion of an ink layer, the downward and upward traveling fluxes lose a small portion of their fluxes in the excitation (lower) wavelength range and gain portions of fluorescently emitted fluxes in the emission (higher) wavelength range. This leads to a differential equation system that can be solved when knowing the boundary conditions.

In order to predict the fluorescent emission spectra of nonbrightened paper printed with invisible fluorescent multi-ink halftones, Hersch *et al.* created a spectral fluorescent emission prediction model relying on the Neugebauer model [18]. This spectral emission prediction model is used to create color images visible only under a UV light source.

Yang created a spectral prediction model accounting for the paper fluorescence in single-ink halftone prints [19]. The model relies on Eq. (1) but assumes that the fluorescent brighteners are located on the upper part of the paper and that the emitted fluorescent irradiance is reflected once by the paper bulk. Lateral light scattering within the paper is modeled by considering the light fluxes that enter from an ink dot and exit from unprinted paper and vice versa, according to the dot surface coverages and according to a point spread function.

I propose a more precise modeling approach, where the fluorescent brighteners are mixed with the paper, where the multiple internal light reflections between the paper bulk and the print–air interface are accounted for, and where I separately calibrate the mean transmittances of the colorants within the excitation wavelength range, i.e., their contribution to the attenuation of the excitation energy. As a result, my model enables predicting with good accuracy the relative fluorescent emission and the total reflectance of chromatic multi-ink halftones printed on paper with fluorescent additives.

3. Clapper–Yule-Based Spectral Prediction Model for Predicting the Reflectance of Nonfluorescent Halftone Prints

Let us separately model the pure reflectance of color halftone prints [term R_{pure} in Eq. (1)], with an illuminant without UV components, i.e., an illuminant that does induce a fluorescent emission. Among the classical reflectance prediction models [20], only the Clapper–Yule model [9] supports halftones and accounts explicitly for the multiple internal

reflections between the paper bulk and the print–air interface.

For introducing the Clapper–Yule model, I consider a single halftone ink layer with a fractional surface coverage a printed on a coated or calendered paper (Fig. 1). Incident light has the probability a of reaching the paper substrate by passing through ink of transmittance $t(\lambda)$ and a probability $(1 - a)$ of reaching the substrate by traversing an unprinted part of the halftone. Since r_s is the specular reflection at the air–paper interface, only portion $(1 - r_s)$ actually enters the print. The light reaching the paper substrate is attenuated by a factor $(1 - r_s)(1 - a + at(\lambda))$, with $(1 - a + at(\lambda))$ representing the attenuation of light by passing once through the halftone layer. Light is then laterally scattered and diffusely reflected by the paper bulk according to its reflectance $r_g(\lambda)$. Traveling upward, it traverses the print with a portion a traversing the ink and a portion $(1 - a)$ traversing an area free of ink. It is reflected at the print–air interface according to a reflection factor r_i , representing the Fresnel reflectivity integrated over all incident angles. The nonreflected part $(1 - r_i)$ of the light exits. At the first exit, the spectral attenuation of the incident light is therefore $((1 - r_s)r_g(\lambda)(1 - r_i)(1 - a + at(\lambda))^2$. The part reflected at the print–air interface travels downward, is diffusely reflected by the paper, and travels upward again. At the second exit, the spectral attenuation is $(1 - r_s)r_g(\lambda)(1 - r_i)(1 - a + at(\lambda))^2 r_i r_g(1 - a + at^2)$.

With K giving the fraction of specularly reflected light reaching the spectrophotometer and by considering the light emerging after 0, 1, 2, ..., $n - 1$ internal reflections (Fig. 1), we obtain the reflectance

$$\begin{aligned}
 R(\lambda) = & K \cdot r_s + (1 - r_s) \cdot r_g(\lambda) \cdot (1 - r_i) \\
 & \cdot (1 - a + a \cdot t(\lambda))^2 \\
 & \cdot [1 + r_i \cdot r_g(\lambda) \cdot (1 - a + a \cdot t(\lambda)^2) \\
 & + (r_i \cdot r_g(\lambda) \cdot (1 - a + a \cdot t(\lambda)^2))^2 + \dots \\
 & + (r_i \cdot r_g(\lambda) \cdot (1 - a + a \cdot t(\lambda)^2))^{n-1}]. \quad (2)
 \end{aligned}$$

For an infinite number of emergences, Eq. (2) yields a geometric series. We obtain the well-known Clapper–Yule expression for the reflectance of a halftone print:

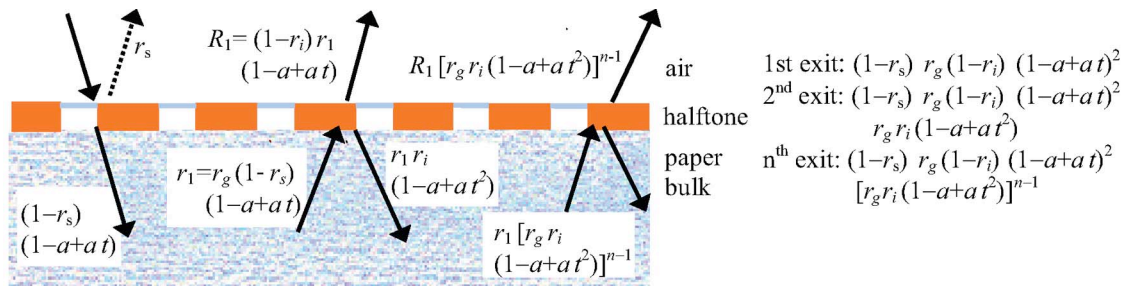


Fig. 1. (Color online) Attenuation of light by multiple reflections within a halftone print.

$$\begin{aligned}
 R(\lambda) = & K \cdot r_s \\
 & + \frac{(1 - r_s) \cdot r_g(\lambda) \cdot (1 - r_i) \cdot (1 - a + a \cdot t(\lambda))^2}{1 - r_g(\lambda) \cdot r_i \cdot (1 - a + a \cdot t(\lambda)^2)}. \quad (3)
 \end{aligned}$$

In the case of paper printed with three independently laid out ink halftone layers such as cyan, magenta, and yellow of respective surface coverage c , m , and y , the surface coverages a_j of the resulting eight basic colorants (known as Neugebauer primaries), i.e., white (a_w), cyan (a_c), magenta (a_m), yellow (a_y), red (a_r), green (a_g), blue (a_b), and black (a_k), are obtained according to the Demichel equations [21,20]:

$$\begin{aligned}
 a_w = & (1 - c) \cdot (1 - m) \cdot (1 - y), \quad a_c = c \cdot (1 - m) \cdot (1 - y), \\
 a_m = & (1 - c) \cdot m \cdot (1 - y), \quad a_y = (1 - c) \cdot (1 - m) \cdot y, \\
 a_r = & (1 - c) \cdot m \cdot y, \quad a_g = c \cdot (1 - m) \cdot y, \\
 a_b = & c \cdot m \cdot (1 - y), \\
 a_k = & c \cdot m \cdot y, \quad (4)
 \end{aligned}$$

The Demichel equations can be extended to four or more inks [5]. By inserting the relative surface coverages of colorants a_j and their transmittances $t_j(\lambda)$ in Eq. (3), we obtain for the predicted reflectance of a color halftone printed with combinations of cyan, magenta, and yellow inks

$$\begin{aligned}
 R(\lambda) = & K \cdot r_s \\
 & + \frac{(1 - r_s) \cdot r_g(\lambda) \cdot (1 - r_i) \cdot \left(\sum_{j=1}^8 a_j \cdot t_j(\lambda) \right)^2}{1 - r_g(\lambda) \cdot r_i \cdot \sum_{j=1}^8 a_j \cdot t_j(\lambda)^2}. \quad (5)
 \end{aligned}$$

Both the specular reflection r_s and the internal reflection r_i at the paper–air interface depend on the refraction indices of the air ($n_0 = 1$) and of the print ($n_1 = 1.53$). Values of r_s and r_i for different indices of refraction are tabulated by Judd [22] and by Emmel [11] for, respectively, Lambertian diffuse light incident on the print and Lambertian diffuse light emerging from the paper bulk and traveling toward the print–air interface.

To put the model into practice, we deduce from Eq. (3) the internal reflectance spectrum r_g of a blank paper by setting the ink surface coverage $a = 0$ and by measuring R_w , the blank paper reflectance:

$$r_g(\lambda) = \frac{R_w(\lambda) - K \cdot r_s}{R_w(\lambda) \cdot r_i - K \cdot r_s \cdot r_i + (1 - r_s) \cdot (1 - r_i)}. \quad (6)$$

We then extract the transmittance of the colorants, i.e., the individual solid inks and solid ink superpositions $t_w(\lambda)$, $t_c(\lambda)$, $t_m(\lambda)$, $t_y(\lambda)$, $t_r(\lambda)$, $t_g(\lambda)$, $t_b(\lambda)$, $t_k(\lambda)$, by inserting into Eq. (3) as $R(\lambda)$ the corresponding measured solid (100%) colorant reflectance $R_j(\lambda)$ and by setting the ink surface coverage $a = 1$:

$$t_j(\lambda) = \sqrt{\frac{R_j(\lambda) - K \cdot r_s}{r_g(\lambda) \cdot r_i \cdot (R_j(\lambda) - K \cdot r_s) + r_g(\lambda) \cdot (1 - r_i) \cdot (1 - r_s)}}. \quad (7)$$

In the Clapper–Yule model, the probability of light to exit from an ink dot is proportional to the ink dot surface coverage, independently if the incident light crosses the print surface through an ink dot or through a white space. This is correct when lateral propagation of light is important in respect to the screen element period. Experiments showed that the Clapper–Yule model makes accurate spectral predictions at screen frequencies equal or larger than 100 lines per inch (coated, calendered, or newsprint paper). At lower screen frequencies, it is necessary to extend the original Clapper–Yule model. A simple extension consists of having a weighted mean between the original Clapper–Yule model and a Saunderson-corrected Neugebauer model [23], i.e., a Neugebauer model [24], where internal reflections between the paper bulk and the print–air interface are accounted for [5]:

$$R(\lambda) = K \cdot r_s + (1 - r_s) \cdot r_g(\lambda) \cdot (1 - r_i) \cdot \left[b \cdot \left[\sum_{j=1}^8 \frac{a_j \cdot t_j(\lambda)^2}{1 - r_i \cdot r_g(\lambda) \cdot t_j(\lambda)^2} \right] + (1 - b) \cdot \frac{\left(\sum_{j=1}^8 a_j \cdot t_j(\lambda) \right)^2}{1 - r_i \cdot r_g(\lambda) \cdot \sum_{j=1}^8 a_j \cdot t_j(\lambda)^2} \right]. \quad (8)$$

The part weighted by $(1 - b)$ is the Clapper–Yule component, and the part weighted by b is the Saunderson-corrected Neugebauer component. Other extensions of the Clapper–Yule model for low-frequency screens exist, e.g., the one proposed by Rogers [4].

4. Ink-Spreading Equations

Equation (5), respectively (8), provides a full spectral reflection prediction model if the effective colorant surface coverages are known. In the general case, however, the nominal ink surface coverages (also

called “digital counts”) are given, from which, according to the Demichel equations [Eq. (4)], only the nominal colorant surface coverages can be deduced. Because of ink spreading (mechanical dot gain), effective ink surface coverages (u_{eff}) are generally larger than the nominal surface coverages (u_{nom}). The effective surface coverage of an ink halftone dot depends on whether it is printed on paper, in superposition with another ink, or in superposition with two inks. It is therefore necessary to establish the ink-spreading curves, i.e., the functions mapping nominal surface coverages to effective surface coverages for each halftone ink in each superposition condition.

In the case of three inks, we have 12 superposition conditions: each ink halftone alone on paper (three curves), each ink halftone on top of another solid ink (two per ink halftone: six curves), and each ink halftone on top of two solid inks (one per ink halftone: three curves). We establish in each superposition condition the function mapping nominal to effective surface coverages. At no surface coverage (0%) and at full surface coverage (solid 100%), nominal and effective surface coverages are identical. We select patches printed at specific nominal surface coverages (e.g., 25%, 50%, and 75%) and fit the corresponding effective surface coverages by minimizing a difference metric such as the sum of the square differences between measured and predicted reflection spectra components. By interpolating between the points ($u_{\text{nom}}, u_{\text{eff}}$) (e.g., linear interpolation), one obtains in each superposition condition s a function $f_s(u_{\text{nom}})$, mapping nominal to effective surface coverages. Figure 2 shows the corresponding dot gain curves, i.e., the effective surface coverage minus the nominal surface coverage as a function of the nominal surface coverage for the cyan, magenta, and yellow inks in each superposition condition. For the three inks, cyan, magenta, and yellow, the superposition conditions are *cyan* alone, cyan superposed with magenta (*c/m*), cyan superposed with yellow (*c/y*), cyan superposed with magenta and yellow (*c/my*), *magenta* alone, magenta superposed with cyan (*m/c*), magenta superposed with yellow (*m/y*), magenta superposed with cyan and yellow (*m/cy*), *yellow* alone, yellow superposed with magenta (*y/m*), yellow superposed with cyan (*y/c*), and yellow superposed with cyan and magenta (*y/cm*).

In order to obtain the effective surface coverages c' , m' , and y' of a color halftone patch, it is necessary for each ink i_u to weigh the contributions of the corresponding mapping functions f_u , $f_{u/v}$, $f_{u/w}$, and $f_{u/vw}$ according to the surface coverages of the corresponding colorants [5].

For the considered system of inks i_c , i_m , and i_y with nominal coverages c , m , and y and effective coverages c' , m' , and y' , assuming that ink halftone dots are printed independently of each other, by computing the relative weight, i.e., the relative surface of each underlying colorant, we obtain the following system of equations:

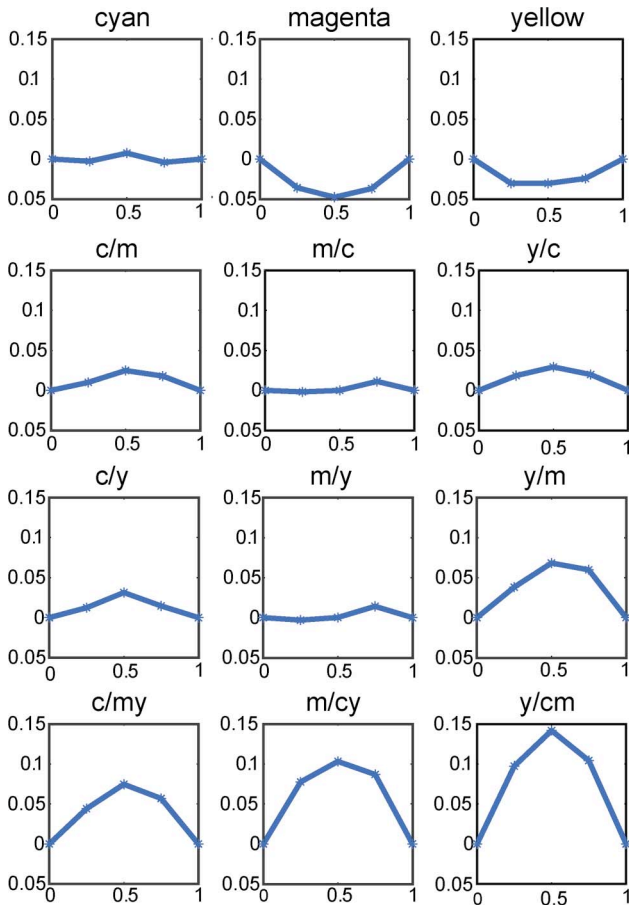


Fig. 2. (Color online) Dot gain curves representing effective minus nominal surface coverages, with effective surface coverages fitted on patches printed at 25, 50, and 75% nominal surface coverages on Canon MP-101 paper with a Canon IP4000 ink jet printer at a screen frequency of 100 lpi.

$$\begin{aligned}
 c' &= f_c(c)(1 - m')(1 - y') + f_{c/m}(c)m'(1 - y') \\
 &\quad + f_{c/y}(c)(1 - m')y' + f_{c/my}(c)m'y', \\
 m' &= f_m(m)(1 - c')(1 - y') + f_{m/c}(m)c'(1 - y') \\
 &\quad + f_{m/y}(m)(1 - c')y' + f_{m/cy}(m)c'y', \\
 y' &= f_y(y)(1 - c')(1 - m') + f_{y/c}(y)c'(1 - m') \\
 &\quad + f_{y/m}(y)(1 - c')m' + f_{y/cm}(y)c'm'. \quad (9)
 \end{aligned}$$

This system of equations is solved iteratively by starting with the initial values of c' , m' , and y' equal to the respective nominal coverages c , m , and y . After a few iterations, the system stabilizes, and the obtained coverages c' , m' , and y' are the effective ink dot surface coverages. The effective colorant coverages, a_w' , a_c' , a_m' , a_y' , a_r' , a_g' , a_b' , and a_k' , are obtained from the effective dot surface coverages c' , m' , and y' of the inks according to the Demichel equations [Eq. (4)]. The complete model comprising ink spreading in all superposition conditions for the cyan, magenta, and yellow inks is illustrated in Fig. 3. The model can be extended to the four cyan, magenta, yellow, and black inks in a straightforward manner [6].

The use of the ink-spreading model together with the spectral prediction model is necessary in order to achieve a high prediction accuracy. Table 1 shows the prediction accuracies for 125 cyan, magenta, and yellow halftone patches. Prediction accuracies are expressed as CIELAB ΔE_{94} color differences between predicted color and measured color calculated from the corresponding reflection spectra. The reference accuracy is based on a single-ink dot gain optimization model [3], noted “single-ink dot gain.” In the present case, accounting for ink spreading improves the mean prediction accuracy by a factor of 2.6.

5. Attenuation of Incoming Light in the Excitation (UV) Wavelength Range

The extended Clapper–Yule model described in Sections 3 and 4 provides an accurate prediction of the reflectance of optically brightened paper under an illuminant whose UV components (e.g., between 320 and 400 nm) have been strongly attenuated by a cut off filter. We start the analysis of the contribution of fluorescent emission by calculating the absorbed energy in the excitation (UV) wavelength range. For this purpose, we first model the attenuation of incoming light in the excitation wavelength range by accounting for both the transmittance of the inks and for the UV light components refracted into the air during the multiple internal reflections.

We first consider a single ink halftone print. As in the Clapper–Yule model, we make the assumption that the halftone ink layer is located on top of the paper bulk (Fig. 4). The paper bulk incorporates the fluorescent additives.

The incident light in the excitation range is $I_u(\lambda)$. It is attenuated by both the specular reflection ($1 - r_s$) at the air–print interface and by the ink halftone layer of surface coverage a and ink transmittance $t_u(\lambda)$. The portion of light ($1 - r_{gu}(\lambda)$) not reflected by the optically brightened paper bulk is absorbed and contributes to the energy inducing the fluorescence. A portion of light $r_{gu}(\lambda)$ is reflected from the paper bulk back toward the ink layer.

The initial traversal through the interface and the ink layer and the absorption by the optically brightened paper ($1 - r_{gu}(\lambda)$) yields the following absorbed irradiance component:

$$I_{u_1}(\lambda) = I_u(\lambda) \cdot (1 - r_s)(1 - a + a \cdot t_u(\lambda))(1 - r_{gu}(\lambda)). \quad (10)$$

As in the Clapper–Yule model, we assume that lateral propagation of light is important in respect to the screen period. Thus light reflected from the paper bulk and then internally reflected at the print–air interface is attenuated by the ink halftone according to its surface coverage. The initial traversal plus one internal reflection composed of a reflection $r_{gu}(\lambda)$ from the paper and a reflection from the halftone print–air interface with attenuation $r_i(1 - a + a t_u^2(\lambda))$ yields the additional absorbed irradiance component

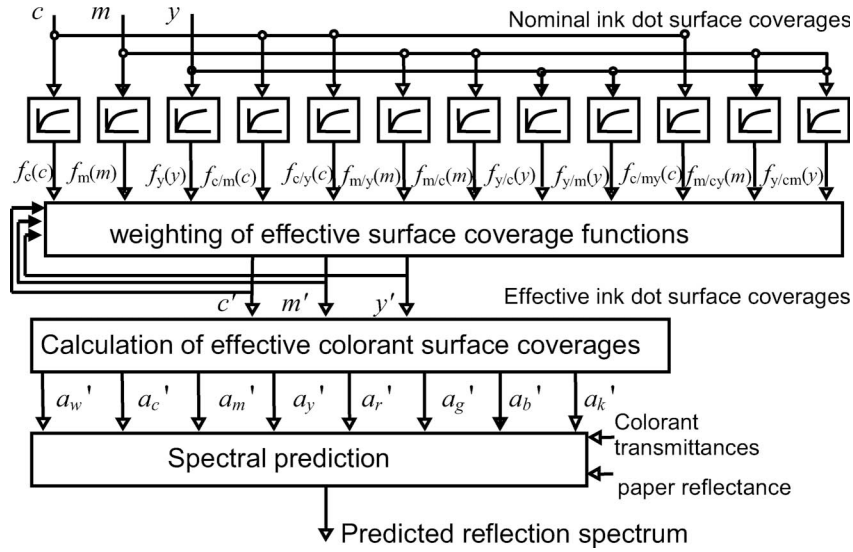


Fig. 3. Spectral prediction model with ink spreading in all superposition conditions.

$$I_{u_2}(\lambda) = I_u(1 - r_s) \cdot (1 - a + a \cdot t_u(\lambda)) \cdot (1 - r_{gu}(\lambda)) \cdot r_{gu}(\lambda) \cdot r_i \cdot (1 - a + a \cdot t_u(\lambda))^2. \quad (11)$$

The initial traversal plus two internal reflections yields the absorbed irradiance component

$$I_{u_3}(\lambda) = I_u(\lambda) \cdot (1 - r_s) \cdot (1 - a + a \cdot t_u(\lambda)) \cdot (1 - r_{gu}(\lambda)) \cdot r_{gu}(\lambda)^2 \cdot r_i^2 \cdot (1 - a + a \cdot t_u(\lambda))^2. \quad (12)$$

The initial traversal plus $n - 1$ internal reflections yields the absorbed irradiance component

$$I_{u_n}(\lambda) = I_u(\lambda) \cdot (1 - r_s) \cdot (1 - a + a \cdot t_u(\lambda)) \cdot (1 - r_{gu}(\lambda)) \cdot r_{gu}(\lambda)^{n-1} \cdot r_i^{n-1} \cdot (1 - a + a \cdot t_u(\lambda))^{n-1}. \quad (13)$$

Summing up, thanks to the geometric series, all irradiance components absorbed by the optically brightened paper within the excitation wavelength range, we obtain

$$I_{\text{abs}}(\lambda) = \sum_{k=1}^{\infty} I_{u_k}(\lambda) = I_u(\lambda) \cdot (1 - r_s) \cdot (1 - a + a \cdot t_u(\lambda)) \cdot (1 - r_{gu}(\lambda)) \times \frac{1}{1 - r_{gu}(\lambda) \cdot r_i \cdot (1 - a + a \cdot t_u(\lambda))^2}. \quad (14)$$

Equation (14), valid for single-ink halftones, can be extended to multiple ink chromatic halftones. When printing a multiple-ink halftone, instead of having only white $(1 - a)$ and one ink dot of surface coverage a and transmittance $t_u(\lambda)$, we have a weighted sum of juxtaposed colorants of transmittances $t_{uj}(\lambda)$, the weights being expressed by the colorant surface coverages a_j . The generalization of Eq. (14) to a color halftone yields

$$I_{\text{abs}}(\lambda) = \sum_{k=1}^{\infty} I_{u_k}(\lambda) = I_u(\lambda) \cdot (1 - r_s) \cdot \left(\sum a_j \cdot t_{uj}(\lambda) \right) \cdot (1 - r_{gu}(\lambda)) \cdot \frac{1}{1 - r_{gu}(\lambda) \cdot r_i \cdot \left(\sum a_j \cdot t_{uj}(\lambda)^2 \right)}. \quad (15)$$

Table 1. Prediction Accuracy Improvement Due to the Ink-Spreading Model with 125 Cyan, Magenta, and Yellow Halftone Patches (CMY) Comprising All Combinations of Nominal Surface Coverages 0, 0.25, 0.5, 0.75, and 1 with UV Illumination Excluded (Canon IP4000 Printer, Screen Frequency 100 lpi, Resolution 600 dpi)

Canon IP4000 100 lpi, MP-101 Paper	Mean ΔE_{94}	95% Quantile ΔE_{94}	Max ΔE_{94}	% of Patches with $\Delta E_{94} > 3$
Single-Ink Dot Gain	2.78	5.18	6.46	44.8
Full-Ink Spreading	1.04	2.21	2.34	0

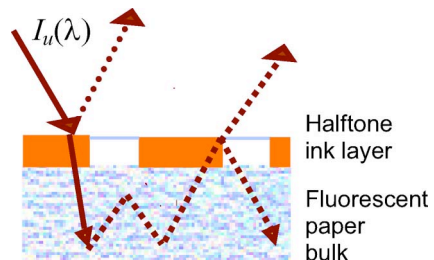


Fig. 4. (Color online) Incoming light within the excitation wavelength range, attenuated by the halftone ink layer, partially reflected by the paper bulk and then partially reflected at the print-air interface.

The halftone colorant surface coverages a_j are the effective surface coverages that can be deduced from the ink-spreading Eq. (9), established under an illuminant excluding the UV component. We assume that the effective colorant surface coverages remain the same independently if the illumination includes or excludes the UV components. This is consistent with the observations of Calabria and Rich [7] who report similar dot gain curves when the UV illuminant is included or excluded.

The absorbed energy E_{abs} , partly used for fluorescent emission, is the integral of the absorbed irradiance over the considered excitation wavelength range ($\lambda_{\text{eInf}}, \lambda_{\text{eSup}}$) ([12], p. 275):

$$E_{\text{abs}} = \int_{\lambda_{\text{eInf}}}^{\lambda_{\text{eSup}}} I_{\text{abs}}(\lambda) \cdot d\lambda = \int_{\lambda_{\text{eInf}}}^{\lambda_{\text{eSup}}} I_u(\lambda) \cdot (1 - r_s) \cdot \left(\sum a_j \cdot t_{uj}(\lambda) \right) \cdot \left(1 - r_{gu}(\lambda) \right) \times \frac{1}{1 - r_{gu}(\lambda) \cdot r_i \cdot \left(\sum a_j \cdot t_{uj}^2(\lambda) \right)} \cdot d\lambda. \quad (16)$$

Both the paper reflectance $r_{gu}(\lambda)$ and the colorant transmittances $t_{uj}(\lambda)$ in the excitation wavelength range are wavelength dependent. Nevertheless, I introduce an equivalent paper reflectance r_{gu}' and equivalent colorant transmittances t_{uj}' , which are constant over the excitation range.

I define the equivalent paper reflectance r_{gu}' as the one yielding the same absorbed energy $E_{\text{abs}P}$ as the original paper reflectance $r_{gu}(\lambda)$ for the unprinted brightened paper:

$$E_{\text{abs}P} = \int_{\lambda_{\text{eInf}}}^{\lambda_{\text{eSup}}} I_u(\lambda) (1 - r_s) \cdot (1 - r_{gu}(\lambda)) \times \frac{1}{1 - r_{gu}(\lambda) \cdot r_i} d\lambda = (1 - r_s) \cdot (1 - r_{gu}') \times \frac{1}{1 - r_{gu}' \cdot r_i} \int_{\lambda_{\text{eInf}}}^{\lambda_{\text{eSup}}} I_u(\lambda) d\lambda. \quad (17)$$

Similarly for each solid colorant J , I define an equivalent ink transmittance t_{uj}' yielding the same absorbed energy $E_{\text{abs}J}$ for the brightened paper printed with that solid colorant:

$$E_{\text{abs}J} = \int_{\lambda_{\text{eInf}}}^{\lambda_{\text{eSup}}} I_u(\lambda) (1 - r_s) \cdot t_{uj}(\lambda) \cdot (1 - r_{gu}') \times \frac{1}{1 - r_{gu}' \cdot r_i \cdot t_{uj}^2(\lambda)} d\lambda = (1 - r_s) \cdot t_{uj}' \cdot (1 - r_{gu}') \frac{1}{1 - r_{gu}' \cdot r_i \cdot (t_{uj}')^2} \times \int_{\lambda_{\text{eInf}}}^{\lambda_{\text{eSup}}} I_u(\lambda) \cdot d\lambda. \quad (18)$$

The equivalent scalar reflectance r_{gu}' and ink transmittances t_{uj}' depend, within the excitation wavelength range, on the wavelength-dependent illuminant spectrum $I_u(\lambda)$, on the brightened paper reflectance $r_{gu}(\lambda)$, and on the solid colorant transmittances $t_{uj}(\lambda)$.

For a halftone print with colorant coverages a_j , we approximate the absorbed energy usable for fluorescent emission by

$$E_{\text{abs}} = (1 - r_s) \cdot \left(\sum a_j \cdot t_{uj}' \right) \cdot (1 - r_{gu}') \times \frac{1}{1 - r_{gu}' \cdot r_i \cdot \left(\sum a_j \cdot t_{uj}'^2 \right)} \cdot \int_{\lambda_{\text{eInf}}}^{\lambda_{\text{eSup}}} I_u(\lambda) \cdot d\lambda. \quad (19)$$

Equation (19) for E_{abs}' is a good approximation of Eq. (16) since the term expressed by the fraction is a second-order term representing absorbed light after one and more internal reflections and since, for each solid colorant J (surface coverages $a_j = 1$ and $a_{k \neq j} = 0$), the absorbed energy is exact. For color halftones, the colorant surface coverages a_j weight the contributions of the different colorants to the reduction in total absorbed energy. With a daylight illuminant such as the NASA standard data of spectral irradiance for the solar disk at the Earth's surface (see [25], pp. 4–6) and with the set of inks and brightened paper described in Section 8, numerical evaluations of Eqs. (16) and (19) show that estimations E_{abs}' do not deviate by more than 1% from the exact values E_{abs} .

6. Calculation of the Emitted Fluorescent Irradiance $I_{\text{em}}(\lambda)$ Exiting from the Print

The fluorescent emission spectrum $F(\lambda)$ of light traveling upward from the fluorescent paper bulk is located within the visible wavelength range and is proportional to the absorbed energy E_{abs}' , with the proportionality constant Q being itself a fraction of the quantum yield ([11], pp. 214–219). The relative shape of the fluorescent emission spectrum $f_{\text{em}}(\lambda)$, nonzero in the visible wavelength range, depends on the fluorescent brighteners added to the paper. Within the visible wavelength range ($\lambda_{\text{vInf}}, \lambda_{\text{vSup}}$), the emission spectrum $f_{\text{em}}(\lambda)$ is normalized:

$$\int_{\lambda_{\text{vInf}}}^{\lambda_{\text{vSup}}} f_{\text{em}}(\lambda) \cdot d\lambda \equiv 1. \quad (20)$$

The fluorescent emission spectrum $F(\lambda)$ emitted by the paper bulk is proportional to $f_{\text{em}}(\lambda)$ and to the absorbed energy E_{abs}' :

$$F(\lambda) = E_{\text{abs}}' Q f_{\text{em}}(\lambda). \quad (21)$$

With Eqs. (21) and (19), let us express the emitted fluorescent spectrum $F(\lambda)$ as a function of the color-

ant surface coverages a_j and the equivalent transmittances t_{uj}' forming the chromatic halftones attenuating the incoming light in the excitation wavelength range:

$$F(a_j, t_{uj}', \lambda) = Q \cdot f_{em}(\lambda) \cdot (1 - r_s) \left(\sum a_j \cdot t_{uj}' \right) \times (1 - r_{gu}') \frac{1}{1 - r_{gu}' r_i \cdot \left(\sum a_j \cdot (t_{uj}')^2 \right)} \cdot \int_{\lambda_{vInf}}^{\lambda_{vSup}} I_u(\lambda) d\lambda. \quad (22)$$

The emitted fluorescent spectrum $F(a_j, t_{uj}', \lambda)$ can be considered as an independent light source illuminating the halftone layer and the print-air interface from below (Fig. 5).

Let us enumerate the exiting emitted fluorescent irradiance components, assuming only a single-ink halftone. The first emitted fluorescent irradiance component traversing the ink halftone and the coating-air interface is

$$I_{e_1}(\lambda) = F(a, t_{uj}', \lambda) \cdot (1 - r_i) \cdot (1 - a + a \cdot t_j(\lambda)), \quad (23)$$

where $t_j(\lambda)$ is the transmittance of the ink in the emission (visible) wavelength range, t_{uj}' is the corresponding equivalent scalar transmittance in the excitation wavelength range, and a is the effective halftone surface coverage.

The second irradiance component undergoes, in addition to the halftone and coating-air interface exit attenuation, one additional internal reflection. Again, assuming that propagation of light is important in respect to the screen element period, such an internal reflection comprises a reflection r_i by the print-air interface, one forward and one backward traversal across the ink halftone with attenuation $(1 - a + a t_j(\lambda)^2)$ and one further reflection $r_g(\lambda)$ by the paper bulk:

$$I_{e_2}(\lambda) = F(a, t_{uj}', \lambda) \cdot (1 - r_i) \cdot (1 - a + a \cdot t_j(\lambda)) \cdot r_g(\lambda) \cdot r_i \cdot (1 - a + a \cdot t_j(\lambda)^2). \quad (24)$$

The third light component is similar to the second, but with one additional internal reflection:

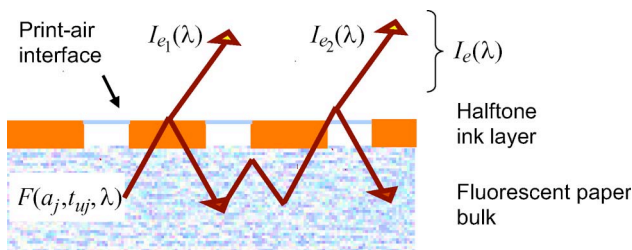


Fig. 5. (Color online) Fluorescent irradiance illuminating the halftone layer and the print-air interface from below.

$$I_{e_3}(\lambda) = F(a, t_{uj}', \lambda) \cdot (1 - r_i) \cdot (1 - a + a \cdot t_j(\lambda)) \cdot r_g(\lambda)^2 \cdot r_i^2 \cdot (1 - a + a \cdot t_j(\lambda)^2)^2. \quad (25)$$

The n th emerging light component is expressed by

$$I_{e_n}(\lambda) = F(a, t_{uj}', \lambda) \cdot (1 - r_i) \cdot (1 - a + a \cdot t_j(\lambda)) \cdot r_g(\lambda)^{n-1} \cdot r_i^{n-1} \cdot (1 - a + a \cdot t_j(\lambda)^2)^{n-1}. \quad (26)$$

The sum of all exiting light components yields a geometric series. We obtain

$$I_e(\lambda) = \sum_{k=1}^{\infty} I_{e_k}(\lambda) = F(a, t_{uj}', \lambda) \cdot (1 - r_i) \cdot (1 - a + a \cdot t_j(\lambda)) \cdot \frac{1}{1 - r_g(\lambda) \cdot r_i \cdot (1 - a + a \cdot t_j(\lambda)^2)}. \quad (27)$$

We can generalize this result to colorant transmittances of a multiple ink halftone:

$$I_{em}(\lambda) = \sum_{k=1}^{\infty} I_{e_k}(\lambda) = F(a_j, t_{uj}', \lambda) \cdot (1 - r_i) \cdot \left(\sum a_j \cdot t_j(\lambda) \right) \cdot \frac{1}{1 - r_g(\lambda) \cdot r_i \cdot \left(\sum a_j \cdot t_j(\lambda)^2 \right)}. \quad (28)$$

Note that in Eq. (28) the surface coverages a_j are the same as in Eq. (22), but the colorant transmittances $t_j(\lambda)$ are the transmittances in the wavelength range of the fluorescent emission spectrum $F(\lambda)$, i.e., in the visible domain.

7. Reflectance of Print with and without Illuminant in the Excitation Wavelength Range (UV)

My goal is to predict the total reflectance of a color halftone printed on paper with fluorescent additives by calibrating the prediction model with the reflectances of chromatic halftone prints under two illuminants, one illuminant excluding and one illuminant including the light components in the excitation wavelength range (UV). Thanks to these measurements, I try to deduce the unknown wavelength-dependent terms of Eq. (22) grouped into the “potential fluorescent emission spectrum” $E_n(\lambda)$, i.e., the spectrum of the emitted fluorescent light if there would be no attenuation by the air-print and print-air interfaces, by the ink halftones and by the paper bulk:

$$E_n(\lambda) = Q \cdot f_{em}(\lambda) \cdot \int_{\lambda_{UVInf}}^{\lambda_{UVSup}} I_u(\lambda) d\lambda. \quad (29)$$

According to Eq. (1), the total spectral reflectance of a print whose paper bulk incorporates fluorescent brighteners and which is illuminated by a light source with UV components can be expressed by

$$R_{UV+V}(\lambda) = \frac{I_{em}(\lambda)}{I_0(\lambda)} + \frac{I_r(\lambda)}{I_0(\lambda)} = \frac{I_{em}(\lambda)}{I_0(\lambda)} + R_V(\lambda), \quad (30)$$

where $I_{em}(\lambda)$ is the emitted fluorescent light exiting the print [Eq. (28)], $I_r(\lambda)$ is the light component reflected by the print, and $I_0(\lambda)$ is the incident light. The ratio $I_r(\lambda)/I_0(\lambda) = R_V(\lambda)$ represents the reflectance of the same print when illuminated by a light source without components in the excitation wavelength range (pure reflectance).

From Eqs. (28), (22), and (29), we obtain for the first part of Eq. (30), i.e., for the fluorescent emission relative to the incident irradiance,

$$\frac{I_{em}(\lambda)}{I_0(\lambda)} = \frac{E_n(\lambda)}{I_0(\lambda)} \cdot \frac{(1-r_s)(1-r_{gu}') \left(\sum a_j \cdot t_{uj}' \right)}{1-r_{gu}'r_i \cdot \left(\sum a_j \cdot (t_{uj}')^2 \right)} \cdot \frac{(1-r_i) \cdot \left(\sum a_j \cdot t_j(\lambda) \right)}{1-r_g(\lambda) \cdot r_i \cdot \left(\sum a_j \cdot t_j(\lambda)^2 \right)}. \quad (31)$$

In Eq. (31), the ratio $E_n(\lambda)/I_0(\lambda)$ is unknown. It can, however, be deduced from reflectance measurements of specific patches, with and without UV illumination. From Eq. (30) we obtain for the component of total reflectance contributed by fluorescent emission

$$\frac{I_{em}(\lambda)}{I_0(\lambda)} = R_{UV+V}(\lambda) - \frac{I_r(\lambda)}{I_0(\lambda)} = R_{UV+V}(\lambda) - R_V(\lambda), \quad (32)$$

and with Eq. (31)

$$\frac{E_n(\lambda)}{I_0(\lambda)} = (R_{UV+V}(\lambda) - R_V(\lambda)) \cdot \frac{1-r_{gu}'r_i \cdot \left(\sum a_j \cdot (t_{uj}')^2 \right)}{(1-r_s)(1-r_{gu}') \left(\sum a_j \cdot t_{uj}' \right)} \cdot \frac{1-r_g(\lambda) \cdot r_i \cdot \left(\sum a_j \cdot t_j(\lambda)^2 \right)}{(1-r_i) \cdot \left(\sum a_j \cdot t_j(\lambda) \right)}. \quad (33)$$

We can, for example, deduce the ratio $E_n(\lambda)/I_0(\lambda)$ from reflectance measurements $R_{pUV+V}(\lambda)$ and $R_{pV}(\lambda)$ of the unprinted brightened paper with and without UV illumination. In this case, the surface coverages a_i of all colorants besides paper white is zero, and the transmittance of the paper white colorant is one. For unprinted brightened paper, Eq. (33) reduces to

$$\frac{E_n(\lambda)}{I_0(\lambda)} = (R_{pUV+V}(\lambda) - R_{pV}(\lambda)) \cdot \frac{1-r_{gu}'r_i}{(1-r_s)(1-r_{gu}')} \cdot \frac{1-r_g(\lambda) \cdot r_i}{(1-r_i)}. \quad (34)$$

An approximate value for the scalar unknown equivalent paper reflectance r_{gu}' can be obtained

by taking the measured brightened paper reflectance at a suitable wavelength within the excitation wavelength range, for example, at 380 nm, and by deducing the corresponding internal reflectance according to Eq. (6). This wavelength is within the fluorescent brightener excitation spectrum, and at the same time, it is part of the reflection spectra delivered by widely available commercial spectrophotometers (e.g., Gretag-Macbeth i7, X-Rite SpectroEye). Assuming an index of refraction of 1.53 for the paper coating, the Fresnel diffuse internal reflectance r_i is equal to 0.614 [22,11], and the Fresnel specular reflection component r_s for diffuse incident light is 0.096 [11].

In order to obtain the unknown equivalent solid colorant transmittances t_{uj}' in the excitation spectrum (UV), I express the fluorescent emission from paper printed with a solid colorant by setting in Eq. (31) the surface coverage a_j of colorant j to one and of all other colorants to zero. In addition, by inserting formula Eq. (33) into formula (31), we obtain for the fluorescent emission of a solid colorant print relative to the incident illumination:

$$\frac{I_{em}(\lambda)}{I_0(\lambda)} = (R_{pUV+V}(\lambda) - R_{pV}(\lambda)) \cdot \frac{(1-r_{gu}')r_i \cdot t_{uj}'}{1-r_{gu}' \cdot r_i \cdot (t_{uj}')^2} \cdot \frac{(1-r_g(\lambda) \cdot r_i) \cdot t_j(\lambda)}{1-r_g(\lambda) \cdot r_i \cdot t_j(\lambda)^2}. \quad (35)$$

We can also measure $I_{em}(\lambda)/I_0(\lambda)$ according to Eq. (32) as the difference between the measured spectral reflectances with and without UV component. Therefore Eq. (35) enables deriving the equivalent colorant transmittance t_{uj}' in the UV wavelength range by minimizing the sum of square differences between predicted and measured relative fluorescent emission spectra components.

The internal paper reflectance $r_g(\lambda)$, respectively the ink colorant transmittances $t_j(\lambda)$ in the visible wavelength range, are deduced from the Clapper-Yule model Eqs. (6) and (7) by measuring the unprinted paper reflectance, respectively the reflectance of the paper printed with the solid colorants, with an illumination excluding excitation range light components (UV excluded).

The general expression for the total reflectance $R_{UV+V}(\lambda)$ of a color halftone print on optically brightened paper is obtained with Eqs. (30) and (31) and by replacing $E_n(\lambda)/I_0(\lambda)$ according to Eq. (34):

$$R_{UV+V}(\lambda) = (R_{pUV+V}(\lambda) - R_{pV}(\lambda)) \cdot \frac{(1-r_{gu}') \cdot r_i \cdot \sum a_i \cdot t_{ui}'}{1-r_{gu}' \cdot r_i \cdot \left(\sum a_i \cdot (t_{ui}')^2 \right)} \cdot \frac{(1-r_g(\lambda)r_i) \cdot \left(\sum a_i \cdot t_i(\lambda) \right)}{1-r_g(\lambda) \cdot r_i \cdot \left(\sum a_i \cdot t_i(\lambda)^2 \right)} + R_V(\lambda), \quad (36)$$

with $R_V(\lambda)$ being the measured or predicted reflectance without excitation range illumination

component. Thanks to Eq. (36), we can predict the reflectance of a color halftone print on a fluorescent diffusing substrate. In Section 8, I present the achieved prediction accuracies.

8. Results and Prediction Accuracy

All measured reflection spectra are obtained with a Gretag-Macbeth i7 spectrophotometer, according to the (de: 8°) geometry, i.e., diffuse illumination with the specular component excluded and a 8° radiance capture [26]. Two illuminants are available: one that includes and one that excludes the UV light components. The corresponding illuminant spectra are shown in Fig. 6. CIELAB coordinates are derived from CIE-XYZ values calculated with a D65 standard illuminant and the CIE 1931 2° standard observer. The color patches are printed with a Canon IP4000 inkjet printer on a Canon MP-101 matte optically brightened paper at a screen frequency of 100 lpi and a resolution of 600 dpi, with classical mutually rotated clustered dot screens. This optically brightened paper is moderately fluorescent, with a reflectance peak of 1.22 at 440 nm.

Let us first qualitatively examine the impact of fluorescence on the paper white and on the solid colorant prints. Figure 7 clearly shows that, for the unprinted brightened paper *white*, there is a very strong difference in reflectance if the brightened paper is illuminated with light comprising components in the excitation wavelength range (UV) or not (CIE-LAB difference $\Delta E_{94} = 11.28$). The fluorescent emission is much smaller for the solid cyan and magenta prints (cyan, $\Delta E_{94} = 0.95$; magenta, $\Delta E_{94} = 0.92$). For the yellow print, there is nearly no fluorescent emission ($\Delta E_{94} = 0.12$). According to the model developed in the previous sections, the strong decrease in fluorescent emission is due either to the absorption of the inks in the excitation wavelength range or to the absorption of the light emitted by paper fluorescence or to both factors. The strong reduction in fluorescent emission for solid colorants suggests that paper fluorescence has the greatest impact on white and on highlight colors created by halftone dots of small and midsize ink surface coverages.

The present section aims (1) at verifying the accuracy of the spectral prediction model accounting for paper fluorescence and (2) at analyzing to what extent a classical spectral prediction model such as the Clapper–Yule model might be sufficient to predict the color of halftones printed on optically brightened paper.

A. UV Fluorescent Emission Prediction

We can verify the accuracy of the fluorescent emission prediction by comparing the measured reflection spectrum R_{V+UV} under an illuminant with UV components and the same reflection spectrum predicted according to the right part of Eq. (36), where R_V is the measured reflection spectrum with an illuminant without UV components. Measured and predicted reflection spectra are converted to CIELAB, and as a

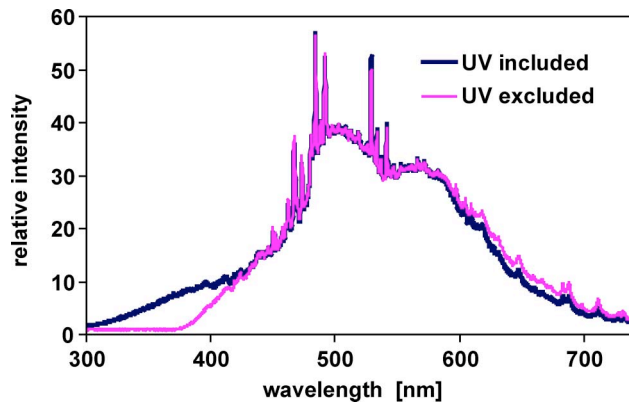


Fig. 6. (Color online) Emission spectra of the two illuminants, UV included and UV excluded, present in the Gretag-Macbeth i7 spectrophotometer.

measure of accuracy, the ΔE_{94} color difference is computed between them. The 125 cyan, magenta, and yellow patches comprise all variations of surface coverages 0, 0.25, 0.5, 0.75, and 1. The fluorescence prediction framework relies on the multiple light reflection process described in Sections 5 and 6. Effective colorant surface coverages are deduced from the ink-spreading extension of the Clapper–Yule model under the illuminant excluding UV components (Section 4). At 380 nm, the measured paper reflectance under the UV included illuminant is 0.140, and the corresponding internal reflectance Eq. (6), used as apparent paper reflectance, becomes $r_{gu}' = 0.310$. Values fitted according to Eq. (35) for the equivalent scalar colorant transmittances are $t_{u\text{Cyan}}' = 0.238$, $t_{u\text{Magenta}}' = 0.186$, and $t_{u\text{Yellow}}' = 0.0764$. The equivalent transmittances of colorants formed by ink superpositions, i.e., red, green, blue, and chromatic black are fitted as zero (lowest limit constraint). These solid colorants completely absorb the excitation wavelength components of the illuminant. This is consistent with the fact that within the precision of the measuring instrument (Gretag-Mac-

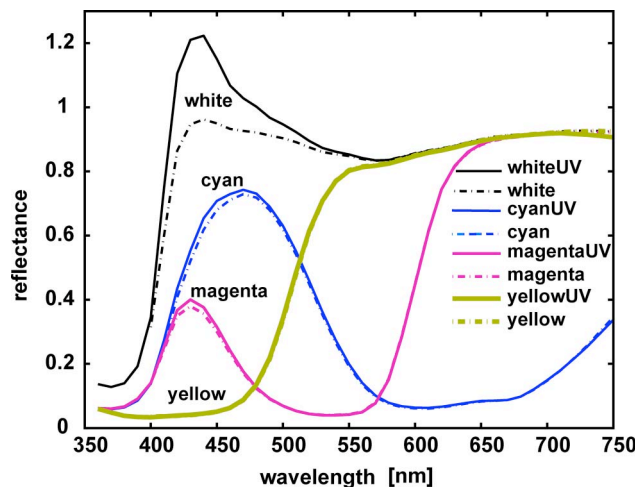


Fig. 7. (Color online) Measured reflectances of paper white and of solid cyan, magenta, and yellow patches under illuminants with and without UV component as a function of wavelength (nm).

both i7 spectrophotometer), the reflectances of the red, green, blue, and black solid colorants do not show any difference between measurements with UV included or UV excluded illuminants.

Table 2 gives the mean prediction accuracy for the 125 cyan, magenta, and yellow patches with all combinations of nominal ink surface coverages 0, 0.25, 0.5, 0.75, and 1. As shown by the mean, 95% quantile and maximal ΔE_{94} colorimetric distance between predicted and measured spectra, the proposed fluorescence model relying on multiple reflections of incident light in the excitation wavelength range and of multiple reflections of light emitted by fluorescence yields very precise results.

B. General Spectral Prediction Accounting for Paper Fluorescence

In Subsection 8.A, I specifically characterized the prediction accuracy of the relative fluorescent emission spectrum $I_{em}(\lambda)/I_0(\lambda)$. Let us now, according to Eq. (36), characterize the precision of the prediction of the total spectral reflectance, with the pure reflectance part R_V predicted according to the ink-spreading-enhanced Clapper–Yule model. The overall total reflectance prediction (Table 3, Line C) cannot be more accurate than the pure reflectance prediction without UV components (Line A). As a comparative figure, we also show in Table 3, Line B, the spectral prediction accuracy that is attained by calibrating the ink-spreading-enhanced Clapper–Yule model with the measured total reflectances, with an illuminant incorporating light components within the excitation wavelength range (UV included).

Interestingly, the total reflectance prediction (Table 3, Line C) obtained with the combined fluorescence and Clapper–Yule model (for predicting R_V) according to Eq. (36) is slightly less accurate than when simply using the ink-spreading-enhanced Clapper–Yule model calibrated with total reflectance values. This is due to the fact that in halftones printed on moderately fluorescent paper, with a white surface coverage of less than 0.125, the influence of fluorescence becomes negligible, but nevertheless the fluorescence prediction introduces an additional mean error of $\Delta E_{94} = 0.42$.

However, in the case of halftones with a significant surface coverage of brightened paper white, the fluorescent model combined according to Eq. (36) with the Clapper–Yule model for predicting R_V yields a significant improvement in prediction accuracy. Table 4 shows the respective prediction accuracies for 27 halftone samples comprising all combinations of 0, 0.25, and 0.5 cyan, magenta, and yellow surface coverages. For this category of halftones, thanks to the prediction of the fluorescent emission spectrum, the mean prediction accuracy is improved by 33%.

Let us gain more insight into the benefits of using the fluorescence model to predict halftones that incorporate a significant portion of unprinted optically brightened paper. As an example, we examine the re-

Table 2. Prediction Accuracy of the Fluorescent Emission Component of a Spectral Reflectance with an Illuminant including UV Components (Gretag-Macbeth i7 Table Spectrophotometer with a d/6° Geometry)

Canon IP4000 100 lpi, MP-101 Paper, Illuminant with UV included, 125 Patches	95%		
	Mean ΔE_{94}	Quantile ΔE_{94}	Max ΔE_{94}
Fluorescent Emission Model	0.418	0.812	0.972

flexion spectra of a color halftone patch of nominal ink surface coverages $cm_y = \{0, 0.25, 0.5\}$. According to the Demichel equations [Eq. (4)], we obtain the corresponding nominal surface coverage of paper white $a_w = 0.75 \times 0.5 = 0.375$. For this halftone, the accuracy of the fluorescent emission component of the total spectral reflectance is $\Delta E_{94} = 0.48$. The total reflectance prediction accuracy obtained by combining the fluorescence prediction and the Clapper–Yule model is $\Delta E_{94} = 0.82$. The reflectance prediction obtained with the Clapper–Yule only is $\Delta E_{94} = 1.44$. The corresponding reflectance spectra are shown in Fig. 8.

Figure 8 clearly shows that the reflection spectrum predicted according to the Clapper–Yule model only is too low at the paper’s fluorescent emission wavelength range (410 to 500 nm). This is due to the fact that the internal paper reflectance deduced according to Eq. (6) is too high within that range (above 1) and that the transmittances of the inks deduced according to Eq. (7) are too low. In halftone patches having an unprinted paper component, light entering the paper and exiting from the ink dot is too much attenuated, yielding a too low reflectance prediction within the paper’s fluorescent emission wavelength range.

9. Conclusions

I propose a model for predicting the fluorescent emission and the total reflectance of colors printed on optically brightened paper. The fluorescent emission prediction model part accounts for both the attenuation of light by the halftone within the excitation wavelength range and for the attenuation of the fluorescent emission by the same halftone within the emission wavelength range. For both the incident light within the excitation wavelength range and for the light emitted by paper fluorescence, the multiple reflections between the paper bulk and the print–air interface are accounted for.

Table 3. Comparison of Prediction Accuracies

Canon IP4000 100 lpi, MP-101 Paper, 125 Patches	95%		
	Mean ΔE_{94}	Quantile ΔE_{94}	Max ΔE_{94}
A: Clapper–Yule, Illuminant without UV Components	1.036	2.211	2.339
B: Clapper–Yule, Illuminant with UV Components	1.132	2.183	2.840
C: Fluorescence Model + Clapper–Yule Model for Predicting R_V	1.248	2.452	2.850

Table 4. Comparison of Prediction Accuracies for 27 Halftones Samples Comprising All Combinations of 0, 0.25, and 0.5 CMY Surface Coverages

Canon IP4000 100 lpi, MP-101 Paper, 27 Patches with CMY Halftones up to 0.5 Surface Coverages	Mean ΔE_{94}	95% Quantile ΔE_{94}	Max ΔE_{94}
A: Clapper–Yule, Illuminant	1.378	2.326	2.840
with UV Components			
B: Fluorescence Model + Clapper–Yule Model for Predicting R_V	1.035	1.782	2.160

The calibration of the fluorescent emission model requires, within the excitation spectrum, the determination of the equivalent internal brightened paper reflectance r_{gu}' and the fitting of the equivalent colorant transmittances t_{uj}' for each colorant J . These values are obtained by measuring the total reflectance (UV included) and the pure reflectance (UV excluded) of the unprinted brightened paper and of each of the colorants, i.e., the solid inks and ink superpositions. The calibration also requires us to calculate the same parameters as the ones for the Clapper–Yule model, namely, the internal paper reflectance $r_g(\lambda)$ and the transmittance of the colorants $t_j(\lambda)$ within the fluorescent emission wavelength range (visible domain). The calibration of a three-ink model with its eight colorants requires therefore 16 spectral measurements.

With such a calibrated fluorescent emission model, it is already possible to predict the fluorescent emission component within the total reflectance for any halftone. More specifically, one may predict the shape and the volume of the full printable color gamut for a given fluorescent substrate and a given set of inks.

By further calibrating the ink-spreading functions mapping nominal ink surface coverages to effective ink surface coverages under an illuminant excluding UV, we can derive for each given set of nominal ink surface coverages the corresponding effective colorant surface coverages a_j . This enables predicting both the corresponding fluorescent emission spectrum and the total reflectance of a halftone printed on optically brightened paper.

The new total reflectance prediction model combines the proposed fluorescent emission prediction and the pure reflectance prediction by the Clapper–Yule model. For 125 cyan, magenta, and yellow halftones comprising all combinations of surface coverages 0, 0.25, 0.5, 0.75, and 1, it reaches a mean prediction accuracy of $\Delta E_{94} = 1.25$ under a D65 standard illuminant. The present analysis shows that for halftones printed with less than 12% of white on moderately fluorescent paper, the effect of fluorescent emission becomes insignificant. For halftones incorporating at least a small surface of paper white, e.g., combinations of *cm*y surface coverages of 0, 0.25, and 0.5, an improved mean prediction accuracy of $\Delta E_{94} = 1.03$ is achieved.

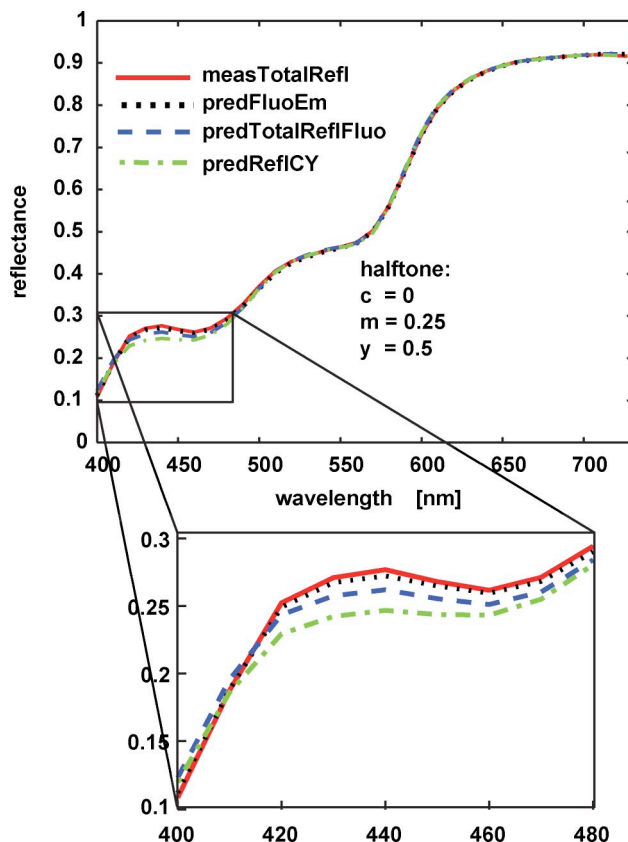


Fig. 8. (Color online) Measured total reflectance (measTotalRefl), predicted fluorescent emission (predFluoEm), predicted total reflectance with the fluorescence model (predTotalReflFluo), and reflectance predicted with the Clapper–Yule model only (predReflCY) for a halftone printed on the MP-101 brightened paper at nominal surface coverages $c = 0$, $m = 0.25$, and $y = 0.5$.

The present spectral prediction model for color prints on optically brightened paper is useful for a number of purposes. First it may help in creating improved printer characterization tables for color management purposes, especially in respect to highlight tones. Second it may enable manufacturers of fluorescent paper to rapidly evaluate the benefits of different fluorescent additives. Third it may help manufacturers of inks in making decisions if a given ink should be more or less absorbent in the UV wavelength range. Finally the prediction of relative fluorescent emission may help in creating embedded watermarks visible only under UV light [27]. The model can be easily used in practice since it requires only reflectance measurements in the visible wavelength range, which may be carried out with commercially available desktop instruments.

One future challenge includes the development of a spectral prediction model that would be independent of the illuminant, for example, by relying on the Donaldson fluorescence matrix, enabling computing the intensity of the emitted spectrum for each excitation wavelength. One further challenge would be the elaboration of a spectral prediction model supporting both the fluorescence of paper and the fluorescence of inks and possibly taking into account

quenching effects, which occur when the concentration of fluorescent molecules becomes too high.

I thank M. Brichon, J. Andres, and B. Gallinet for their efforts in measuring fluorescent samples. Many thanks also to M. Hebert and B. Dwir, both from Ecole Polytechnique Fédérale de Lausanne, for their advice in respect to fluorescence measurements. This project has been partly funded by the Swiss National Science Foundation (SNSF), grant 200020-105119.

References

1. J. A.S. Viggiano, "Modeling the color of multi-colored halftones," Proc. TAGA 44–62 (1990).
2. K. Iino and R. S. Berns, "Building color management modules using linear optimization I. Desktop," J. Imaging Sci. Technol. **42**, 79–94 (1998).
3. R. Balasubramanian, "Optimization of the spectral Neugebauer model for printer characterization," J. Electron. Imaging **8**, 156–166 (1999).
4. G. Rogers, "A generalized Clapper–Yule model of halftone reflectance," Color Res. Appl. **25**, 402–407 (2000).
5. R. D. Hersch, P. Emmel, F. Crété, and F. Collaud, "Spectral reflection and dot surface prediction models for color halftone prints," J. Electron. Imaging **14**, 033001 (2005).
6. T. Bugnon, M. Brichon, and R. D. Hersch, "Model-based deduction of CMYK surface coverages from visible and infrared spectral measurements of halftone prints," Proc. SPIE **6493**, 649310 (2007).
7. A. J. Calabria and D. C. Rich, "Brigher is better? Investigating spectral color prediction of ink on optically brightened substrate," *Proceedings IS&T/SID 11th Color Imaging Conference* (Society for Imaging Science and Technology, 2003), pp. 288–293.
8. International Color Consortium, "The effects of fluorescence in the characterization of imaging media," Summary of CIE Publication 163, www.icc.org.
9. F. R. Clapper and J. A. C. Yule, "The effect of multiple internal reflections on the densities of halftone prints on paper," J. Opt. Soc. Am. **43**, 600–603 (1953).
10. K. Nassau, *The Physics and Chemistry of Color* (Wiley, 1983).
11. P. Emmel, "Physical models for color prediction," in *Digital Color Imaging*, G. Sharma, ed. (CRC, 2003), pp. 173–238.
12. F. Grum, "Colorimetry of fluorescent materials," in *Optical Radiation Measurements, Volume 2, Color Measurements*, F. Grum and C. J. Bartelson, eds. (Academic, 1980), pp. 235–288.
13. R. Donaldson, "Spectrophotometry of fluorescent pigments," Br. J. Appl. Phys. **5**, 210–214 (1954).
14. E. Allen, "Separation of the spectral radiance factor curve of fluorescent substrates into reflected and fluoresced components," Appl. Opt. **12**, 289–293 (1973).
15. P. Emmel and R. D. Hersch, "Spectral prediction model for a transparent fluorescent ink on paper," in *Proceedings IS&T/SID 6th Color Imaging Conference* (Society for Imaging Science and Technology, 1998), pp. 116–122.
16. T. Shakespeare and J. Shakespeare, "A fluorescent extension to the Kubelka–Munk model," Color Res. Appl. **28**, 4–14 (2003).
17. G. L. Rogers, "Spectral model of a fluorescent ink halftone," J. Opt. Soc. Am. A **17**, 1975–1981 (2000).
18. R. D. Hersch, P. Donzé, and S. Chosson, "Color images visible under UV light," Proc. SIGGRAPH 2007, ACM Trans. Graph. **26** (3), Article 75, 1–9 (2007).
19. L. Yang, "Spectral model of halftone on a fluorescent substrate," J. Imaging Sci. Technol. **49**, 179–184 (2005).
20. D. R. Wyble and R. S. Berns, "A critical review of spectral models applied to binary color printing," Color Res. Appl. **25**, 4–19 (2000).
21. M. E. Demichel, Procédé **26**, 17–21 (1924).
22. D. B. Judd, "Fresnel reflection of diffusely incident light," J. Res. Natl. Bur. Stand. (U.S.) **29**, 329–332 (1942).
23. J. L. Saunderson, "Calculation of the color pigmented plastics," J. Opt. Soc. Am. **32**, 727–736 (1942).
24. H. E. J. Neugebauer, "The theoretical basis of multicolor letterpress printing," Color Res. Appl. **30**, 322–331 (2005).
25. G. Wyszecki and W. S. Stiles, *Color Science: Concepts and Methods, Quantitative Data and Formulae*, 2nd ed. (Wiley, 1982), Table 1(1.2.1), pp. 4–6.
26. In all equations, the attenuation of light exiting through the print–air interface is modeled by the Fresnel diffuse transmittance term $(1 - r_i)$. When performing measurements, this would imply that an integrated sphere is used to capture all exiting irradiance components. If a measurement instrument is used that captures the exiting radiance perpendicularly ($\theta = 0^\circ$) or at a small angle ($\theta = 8^\circ$), the exit attenuation term $(1 - r_i) = 0.386$ appearing in Eqs. (2), (3), (5)–(8), (23)–(28), (31), (33), and (34) should, according to radiometric considerations, be replaced by the attenuation of the radiance across the print–air interface due both to Fresnel transmittivity and to cone spreading $(1 - r_s(\theta))/(n_{\text{print}})^2$ in the present case $(1 - 0.0438)/(1.53^2) = 0.408$ (see [28]). However, since both terms are numerically close one to another and since the print–air interface is not perfectly flat, I do not recommend performing these changes. This is consistent with observations by C. Kortüm who did not observe, for diffusely reflecting media, significant reflectance factor differences between collimated $45^\circ/0^\circ$ and integrated sphere $45^\circ/d$ or $d/0^\circ$ measurement geometries [29].
27. R. Bala, R. Eschbach, and Y. Zhao, "Substrate fluorescence: bane or boon?," in *Proceedings IS&T/SID 15th Color Imaging Conference* (Society for Imaging Science and Technology, 2007), pp. 12–17.
28. M. Hebert and R. D. Hersch, "Classical print reflection models: a radiometric approach," J. Imaging Sci. Technol. **48**, 363–374 (2004).
29. G. Kortüm, "Optical geometry of the measurement arrangement," in *Reflectance Spectroscopy* (Springer, 1969), pp. 170–175.